International Journal of Computational Methods
Vol. 17, No. 3 (2020) 1850137 (18 pages)

DOI: 10.1142/S0219876218501372

3D Finite Element Simulation of Shot Peening Using a Sequential Model with Multiple-Shot Impacts

Qin Wei[*,†], Wenxin Wu[†], Wei He[‡], Jianguo Zhu[†,§,‖] and Jian Zhang[†,¶,‖]

[*]*Faculty of Science, Jiangsu University of Science and Technology Zhenjiang, Jiangsu, P. R. China*

[†]*Department of Mechanics and Engineering Science Jiangsu University, Zhenjiang, Jiangsu, P. R. China*

[‡]*AML, Department of Engineering Mechanics Tsinghua University, Beijing 100084, P. R. China*

[§]*zhujg@ujs.edu.cn*

[¶]*jianzhang@ujs.edu.cn*

Received 1 February 2018
Revised 29 May 2018
Accepted 15 July 2018
Published 14 August 2018

A sequential model of multiple-shot impacts has been established to investigate the shot peening process. Shot groups are proposed and designed with different patterns to obtain full surface coverage in the impacted region and a satisfactory computational efficiency. The sequential model was applied for the prediction of residual stress on a GH4169 alloy specimen. The results showed that uniform and saturated states of residual stress along the surface and depth profile were obtained in the impacted region when the numerical order of shot patterns reached 4. Furthermore, the numerical results of compressive residual stress in the subsurface were compared with the experimental results obtained using the X-ray diffraction (XRD) analysis and the incremental hole drilling method. The maximum relative error between the numerical results and XRD measurement was 11.6%. Furthermore, the stress profile measured using the incremental hole drilling method was consistent with the numerical results. The established finite element model demonstrated its robustness and effectiveness for the evaluation of residual stress in the shot-peened GH4169 alloy, and it may be applied to other metallic materials with simple modifications.

Keywords: Finite element simulation; sequential model; residual stress; shot peening.

1. Introduction

The Ni-based alloy, GH4169, has been widely used in aerospace, petroleum, and nuclear industries owing to its excellent fatigue tolerance, high-temperature oxidation resistance, and good machinability [Huang *et al.* (2013)]. In order to obtain

[‖]Corresponding authors.

optimal mechanical properties, the components of GH4169 alloy are often processed using various surface treatment technologies, such as shot peening, sand blasting, and laser shock peening. Compared to other treatment technologies, shot peening has the advantages of low cost and easy implementation. It entails impacting a metal or composite surface with small, hard, and spherical shots to create plastic deformation. The consequent compressive residual stress layer increases the material hardness and retards crack initiation [Liu *et al.* (2012); Ochi *et al.* (2001)].

Numerical analyses of shot peening with finite element (FE) simulation are often used to investigate the mechanism of residual stress formation, including the mechanisms of dynamic impact, work hardening, and microstructural characteristics [Han *et al.* (2000)]. Shot peening simulations can be mainly classified into two categories according to the impacted position of shots: sequential model and random model. In the sequential model, shots impact the target surface at a fixed position and in a fixed order. In the literature, Meguid *et al.* [1999] used FE models to simulate the process of shot peening with a single shot and twin shots. The plastic zone and residual stress distributions induced by impacts of shot were analyzed. The effects of shot parameters, such as shot velocity, size, and shape were also discussed. Majzoobi *et al.* [2005] developed a multiple-shot impact model to study the variation of the in-depth residual stress profile. Their results showed that a uniform state of residual stress can be obtained with the increase in the number of impacts. The corresponding number of shots changed with peening conditions. Frija *et al.* [2006] numerically simulated the shot peening process using the FE method with the mechanism of elastic plastic coupled with damage. The residual stress, plastic deformation profiles, and surface damage were obtained, and they demonstrated consistency with the experimental observations. Hong *et al.* [2008] simulated multiple impacts with a shot stream using a discrete element method. Peening process parameters were analyzed to evaluate the peening quality. Gangaraj *et al.* [2011] presented an FE analysis of shot peening effect on fretting fatigue parameters. The effects of shot peening on normal stress, shear stress, bulk stress, and slip amplitude were investigated. Generally, only several fixed modes were used to simulate patterns of shot impact in sequential models, and residual stress distributions at center points of treated area were mainly concerned.

Owing to the availability of significantly increased computing power [Chen *et al.* (2014)], the random model is proposed to simulate the realistic shot-peening process. In the random model, impacted shots are randomly distributed. There were many studies related to the random FE simulation of shot peening. Miao *et al.* [2009] developed an FE model with multiple randomly distributed shots to simulate the dynamics of the impingement process. Gangaraj *et al.* [2014] presented a random FE simulation to evaluate the surface coverage for each impact. Sanjurjo *et al.* [2014] investigated the effects of a constitutive material model on the residual stress and roughness of a target material. The random model was used to simulate the realistic shot peening process and provided a very accurate prediction of both residual stress and surface roughness. Gangaraj *et al.* [2015] employed a constrained random positioning method for each increment of coverage. The dislocation density was evaluated and the gradient of the resultant grain size was predicted in the surface layers. Ghasemi *et al.* [2016] analyzed the effect of shot peening coverage on the residual stress profile. A simulation of realistic shot peening process was achieved with a satisfactory computational time and without reducing the number of impacts and analysis accuracy. Seddik *et al.* [2017] proposed a simple methodology for optimizing the process parameters of the shot peening surface.

In the previous simulations, surface coverage and impacted intensity were mostly considered for evaluating the reliability and effectiveness of the FE model. According to the realistic shot peening process, random models were commonly recommended. However, complex pre-processing was performed with additional program software, such as MATLAB and Python. There are some specialized methods to deal with large number of random shots, for example Smoothed-particle hydrodynamics [Wang and Liu (2011)]. Moreover, a large number of shots were used in order to obtain full surface coverage, which significantly increased the computation time. However, sequential models are operated with a graphical user interface; thus, there is no necessity of pre-processing using other software. Furthermore, the number of shots is relatively small. Hence, the benefits of sequential models are their simplicity and lower time consumption. However, one of the main challenges of sequential models is the design of shot patterns.

Furthermore, simulation results were usually compared with experiments for the verification of FE models. The residual stresses in shot peening components were often experimentally investigated. X-ray diffraction (XRD) was one of the main techniques used to measure the residual stresses on the surface of the specimen. The XRD was used to measure the shot-peened residual stresses of aluminum alloy A2017-T3 [Soyama and Takeo (2016)], austenitic stainless steels AISI316 [Kumagai *et al.* (2014)], cast iron [Bagherifard *et al.* (2014)] and tungsten cemented carbide [Wang *et al.* (2017)]. Layer removal methods were employed if the residual stress profile was investigated. Hole drilling relaxation combined with a strain-gage rosette was one of the most popular methods for the measurement of residual stress. The relevant standard has been established [ASTM E837 (2008)]. The incremental hole drilling method was used to measure residual stress profile in aluminum alloy 7075 [Valentini *et al.* (2011)], low-alloy steel [Mahmoudi *et al.* (2016)], and medium carbon steel [Sherafatnia *et al.* (2016)].

The aim of the present work is to establish a sequential model with multiple-shot impacts to simulate the shot peening process. The model features diversified patterns of shot impact, so that a high surface coverage and a uniform residual stress can be obtained. First, shot groups are proposed and designed with different patterns to obtain full surface coverage in the impacted region. Furthermore, quantitative relationships between the plastic strain and residual stress are discussed. The results of the numerical simulation are compared with the experimental results obtained using the XRD analysis and the incremental hole drilling method. The modeling approach demonstrates good computational efficiency.

2. Materials and Experimental Procedures

2.1. *Shot peening procedure*

Three cylindrical specimens of GH4169 alloy were machined to a diameter of 60.0 mm with a thickness of 5.0 mm and the treated surfaces were ground softly. After grinding, initial residual stress was measured, and the value of stress was less than 45 MPa. The stress was small enough, and the effect on residual stress distributions induced by shot peening can be negligible. All the specimens were extracted from the same forged bar to ensure similarity of microstructure. Shot peening treatments were performed with S410 stainless steel shots. The average diameter of the shots was 0.8 mm, and the impingement angle was equal to approximately 90°. An air blast machine was used to treat the specimens. The setup parameters were an air pressure of 8 bar, and nozzle diameter of 5 mm. The specimens were induced several successive shot peening treatment in order to obtain full surface coverage. The shot velocity was approximately 60 m/s according to the calibration by the equipment supplier.

2.2. *Residual stress measurement*

The residual stress in the subsurface of specimens was first measured using XRD. The measurements were carried out using an x-350A type XRD device and the $\sin^2 \Psi$ method. The residual stress can be calculated as follows [Noyan and Cohen (1987)]:

$$\sigma = K \cdot \frac{\partial(2\theta)}{\partial(\sin^2 \Psi)}, \tag{1}$$

where K is the stress coefficient of the material and θ is the diffraction angle. The experimental parameters are listed in Table 1.

Furthermore, the residual stress profile along the depth direction was measured using the incremental hole drilling method. A stepped hole with tiny increments was drilled at the center of a type B rosette gage, which was attached onto the treated surface. The surface strain relief ε_j measured after completing the hole-depth j step depends on the residual stress in the specimens contained in all the hole-depth steps

Table 1. Experimental parameters for the XRD measurement.

X-ray supply voltage	20.0 kV	Diffraction angle 2θ	124.00°–132.00°
Miller indices (h k l)	(2 2 0)	Sweep step	0.10°
Φ collimator (mm)	2	Wavelength Kα(Cr)	0.2291 nm
Tilt Ψ (°)	0, 25, 35, 45	Stress coefficient (K)	−601 MPa/°

$1 \leq k \leq j$ [ASTM Standard E837 (2008)]:

$$\varepsilon_j = \frac{1+\nu}{E}\sum_{k=1}^{j}\overline{a}_{jk}((\sigma_x+\sigma_y)/2)_k + \frac{1}{E}\sum_{k=1}^{j}\overline{b}_{jk}((\sigma_x-\sigma_y)/2)_k\cos 2\theta + \frac{1}{E}\sum_{k=1}^{j}\overline{b}_{jk}(\tau_{xy})_k\sin 2\theta, \tag{2}$$

where E is Young's modulus, ν is Poisson's ratio, and θ is the angle of strain gage from the x-axis. The calibration constants $\overline{a}_{jk}$ and $\overline{b}_{jk}$ are defined as the relieved strains in the hole j steps depth owing to the unit stresses within the hole $k$step which can be referred to in ASTM E837.

The incremental volume removal was realized using a self-developed hole drilling equipment shown in Fig. 1. A carbide end mill with the diameter of 2 mm was used as the cutting tool. The Z translation stage was a stepper motor controlled by a programmable logic controller, providing a precision of 6.3 μm in each drilling step along the direction perpendicular to the specimen surface. Each drilling step was 50 μm with strain measurement and a total of 20 equal steps were implemented [Wu *et al.* (2014, 2015)].

3. Finite Element Analysis

A three-dimensional model was developed to simulate the shot peening treatment process using the commercial software ABAQUS/Explicit. The target was a GH4169 alloy specimen in the form of a cuboid with the dimensions of $8 \times 8 \times 4.8\,\text{mm}^3$. The shot (S410) with a diameter of 0.8 mm was assumed to have an isotropic linear elastic property. Eight-node linear brick elements (C3D8R) were used to model the specimen and the shot. A sensitivity study has been carried out to optimize the dimensions of the target surface elements. The element size of the specimen was approximately 50 μm beneath the treated surface and varies gradually to 200 μm at

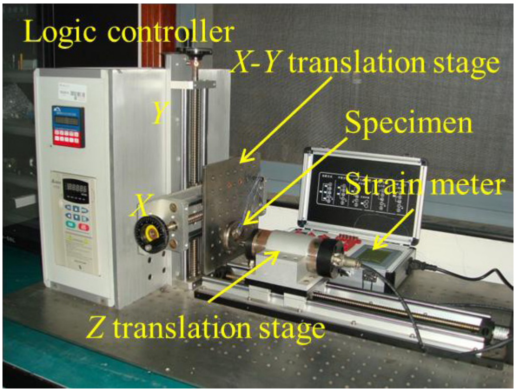

Fig. 1. Self-developed incremental hole-drilling equipment.

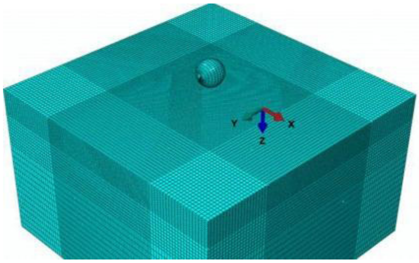

Fig. 2. Finite element meshes of the specimen and shot.

the bottom. The bottom of the specimen was fixed, and some preliminary attempts of numerical simulation were made to avoid the influences of boundary conditions on the numerical outcomes. The initial velocity of the shots was set to 60 m/s along the z-direction according to the experiment. The FE meshes of the specimen and the shot are shown in Fig. 2.

In order to simulate the shot peening process with full coverage, a sequential model with multiple impact shots was developed using the FE method. First, multiple shots with a fixed distribution, or shot group, were established, as shown in Fig. 3. There were several types of shot groups with fixed distributions. The 2-shot group and 3-shot group were designed to sequentially impact the surface four times. Each rotating angle of the 2-shot group and 3-shot group was 45° and 30°, respectively. The 4-shot, 5-shot, and 6-shot groups were designed to impact the surface twice and each rotation angle was 45°, 36°, and 30°, respectively. Second, sequential impact patterns with shot groups, or shot patterns, were proposed to provide adequate overlapping between indentations, as shown in Fig. 4. For n-order shot pattern, it is composed of n-order shot group and $(n-1)$-order shot pattern. For

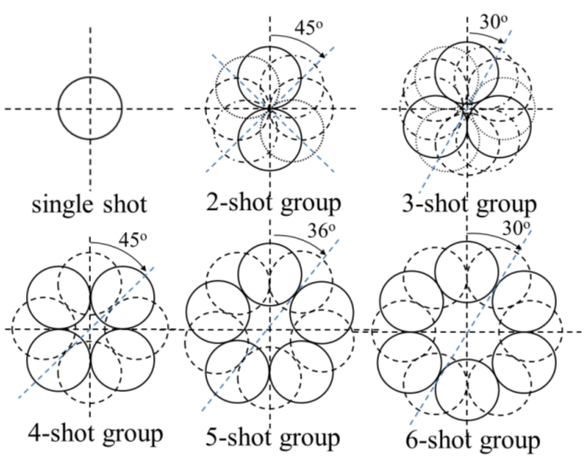

Fig. 3. Schematic of the shot groups.

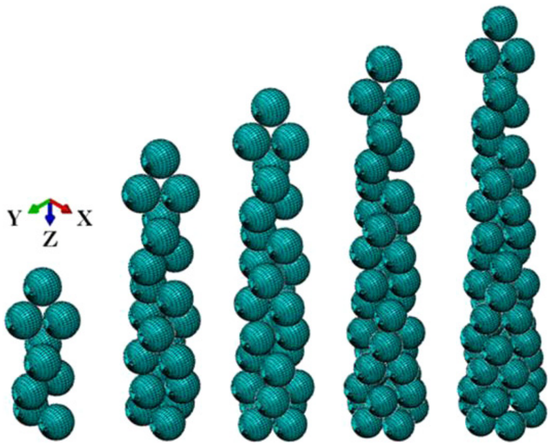

Fig. 4. Schematic of the shot patterns: (a) 2-shot pattern, (b) 3-shot pattern, (c) 4-shot pattern, (d) 5-shot pattern, and (e) 6-shot pattern.

Table 2. Mechanical properties of GH4169 alloy and S410.

Material	Density (kg/m^3)	Elastic modulus (GPa)	Poisson's ratio
GH4169	8240	199.9	0.30
S410	7800	210	0.28

example, the 2-shot pattern was designed to sequentially impact the surface with the 2-shot group and single shot. For 3-shot pattern, the 3-shot group was arranged impacting the surface before 2-shot pattern.

The mechanical properties of the specimen and the shot are listed in Table 2. In order to mimic the plastic behavior of the specimen during treatment, the Johnson–Cook law [Ren *et al.* (2014)] was used:

$$\sigma = (A + B\varepsilon_p^n)[1 + C\ln(\dot{\varepsilon}^*)][1 - (T^*)^m], \tag{3}$$

where σ is the stress flow; ε_p is the effective plastic strain; A, B, n, C, and m are material constants. The parameter $\dot{\varepsilon}^*$ can be determined by the expression $\dot{\varepsilon}^* = \dot{\varepsilon}_p/\dot{\varepsilon}_0$, where $\dot{\varepsilon}_p$ and $\dot{\varepsilon}_0$ are the effective plastic strain rate and reference plastic strain rate, respectively. T^* is the homologous temperature, which can be calculated using the following expression:

$$T^* = (T - T_r)/(T_m - T_r), \tag{4}$$

where T_r and T_m are the reference temperature and melting temperature, respectively. In the shot peening processing, the temperature T of target material is far less than T_m, and T^* can be approximated at zero. $\dot{\varepsilon}_0 = 1s^{-1}$ is used for this study. Herein, the constants for the Johnson–Cook model are listed in Table 3.

Table 3. Material constants of GH4169 [Ren *et al.* (2014)].

Material	A (MPa)	B (MPa)	N	C	m
GH4169	860	1100	0.5	0.0082	1.05

In order to prevent residual oscillations, Rayleigh damping was introduced to the material damping behavior. Eq. (5) defines the damping property where $[C]$ is the damping matrix, $[M]$ is the mass matrix of the model, and $[K]$ is the stiff matrix [Abaqus Analysis User's Manual (2010)].

$$[C] = \alpha[M] + \beta[K], \tag{5}$$

$$\alpha = 2\omega_0\xi. \tag{6}$$

The coefficients α and β are factors proportional to the mass matrix and stiff matrix, respectively. Further, α can be determined using Eq. (6), where ω_0 is the initial frequency and ξ is the damping ratio. Generally, the value of $\xi = 0.5$ is adequate for rapid damping oscillations of low frequency [Meguid *et al.* (2006)]. The frequency ω_0 can be calculated as follows:

$$\omega_0 = \frac{2\pi}{h}\sqrt{\frac{E}{\rho}}, \tag{7}$$

where E is the Young's modulus of material, ρ is its density, and h is the height of the specimen. The contact algorithm between the shot and target surface was defined with a penalty tangential behavior, and the isotropic Coulomb friction coefficient was set to 0.2.

In order to determine an appropriate mass proportional coefficient α, several trial runs were conducted to obtain a reliable value. From Eq. (6), the coefficient α is equal to 6.44×10^6 (s^{-1}). The results show that the residual oscillations could be damped when the coefficient α was considered as 1.28×10^6 (s^{-1}). The coefficient β was set to zero.

4. Results and Discussion

4.1. *FE method simulation results*

The diameter and depth of indentation induced by a single-shot impact was first investigated. Fig. 5 shows the surface displacement (U_z) and equivalent plastic strain (PEEQ) of the indentation profile induced by the single-shot impact. It can be observed that there were some corrugations around the indentation, which were caused by the crimp of the shot. The boundary of the indentation was determined when the Z-displacement was zero, as indicated by points A and B. It can be observed that the radius (r) and depth of the indentation (h) were $165\,\mu$m and $28\,\mu$m, respectively. Furthermore, the value of PEEQ at points A or B is equal

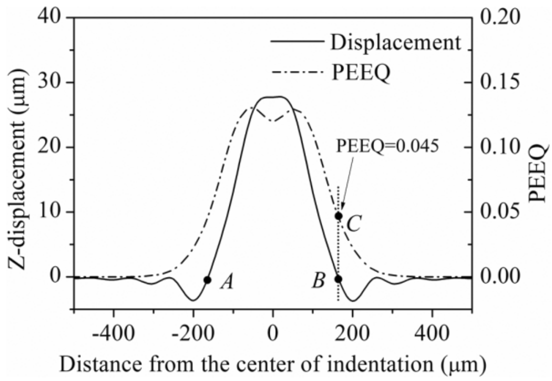

Fig. 5. Indentation profile of a single-shot impact.

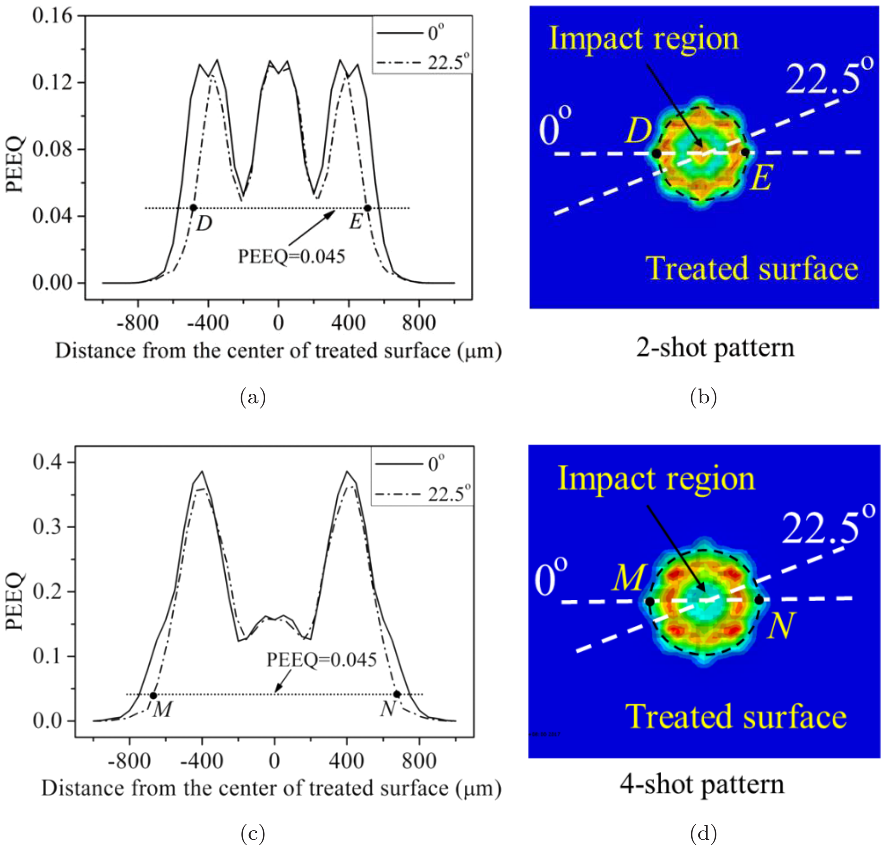

Fig. 6. PEEQ distributions along two lines on the treated surface: (a) PEEQ distribution of 2-shot pattern, (b) coverage of impact region for 2-shot pattern, (c) PEEQ distribution of 4-shot pattern, and (d) coverage of impact region for 4-shot pattern.

to 0.045. Therefore, the impacted region can also be defined as the region on the treated surface when the value of PEEQ is larger than 0.045 [Miao *et al.* (2009)]. Furthermore, the impacted region of multiple impacts can be determined conveniently according to the calculated distribution of PEEQ, and thus, the surface coverage can be evaluated in the following study of multiple impacts.

Figure 6 shows the PEEQ distributions and impact region sketches of the 2-shot and 4-shot pattern on the treated surface. For the 2-shot pattern, there are 9 indentations in the impacted region. As shown in Figs. 6(a) and 6(b), two lines with angles of 0° and 22.5° to the x-axis are the directions of the maximum and minimum diameters of the impacted region, respectively. The impacted region is the circular region between points D and E as their values of PEEQ are greater than 0.045. Therefore, the radius of the impacted region is 490 μm. Similarly, as shown in Figs. 6(c) and 6(d), the boundaries of the 4-shot pattern can be represented by points M and N, and the radius of the impacted region is 670 μm. The area of the impacted region increases with the numerical order of shot patterns. Moreover, the maximum value of PEEQ in the impacted region increases, from 0.125 in the 2-shot pattern to 0.38 in the 4-shot pattern.

A percentage of coverage greater than 98% is considered full coverage [SAE Standard J2277 (2003)]. The percentage of coverage evaluated using the distribution of PEEQ was used in present simulation [Miao *et al.* (2009)]. Herein, the coverage was approximated as the ratio of the number of nodes with accumulated plastic strain (PEEQ) greater than threshold value, to the total number of nodes on the representative surface. Considering the 2-shot pattern as an example, the PEEQ value of the total nodes in the impacted region is larger than threshold value of 0.045. Hence, it can be concluded that the coverage of the 2-shot pattern in the impacted region reaches 100%. The same evaluation method is applied to analyze the simulation results of the other model. The radii of the impacted surface for full coverage are presented in Table 4. It can be observed that the radius of impacted region for the 3-shot pattern is approximately 3.69 times the radius of indentation. However, with regard to the 4-shot pattern, the radius of the impacted region is only 4.07 times the radius of indentation. The radius of the impacted region slowly increases with the numerical order of shot patterns. This is due to the dual impacts

Table 4. Radii of the impacted surface and surface coverage of shot patterns.

Pattern	Number of shots	Radius of impacted region (μm)	Surface coverage (%)
1-shot pattern	1	165 (1.00r)	100
2-shot pattern	9	490 (2.97r)	100
3-shot pattern	21	608 (3.69r)	100
4-shot pattern	29	671 (4.07r)	100
5-shot pattern	39	706 (4.28r)	100
6-shot pattern	51	810 (4.91r)	100

Note: r is the radius of impacted surface of 1-shot pattern.

for the 4-shot, 5-shot, and 6-shot groups. Although the radius of the impacted region can be increased by increasing the impact time for the shot groups, this operation leads to a sharp rise in the total number of shots and the computational costs. When surface coverage of the simulation and experiment both reach 98%, the residual stress of numerical simulation can be compared with the experimental results.

The area of impacted surface can have a significant effect on the numerical results of the shot peening process [Gangaraj *et al.* (2014)]. In previous sequential models of multiple impacts, symmetry boundary conditions were usually used to investigate the influence of impacts at adjacent locations. In the symmetry cell models of Meguid *et al.* [2002] and Kim *et al.* [2010], a single shot was assigned to impact four corners of the cell several times. Majzoobi *et al.* [2005] used single shot, 2-shot, and 4-shot groups to impact the surface sequentially. However, the symmetry boundary conditions in the above models limited the area of the processed surface, and the effect of impacts far from the boundary was ignored, which led to a uniform tendency of stress distribution. As mentioned before, although the simulations of random impact can provide adequate surface area for shot peening, the number of random shots and the computational costs rapidly increase with the area of the

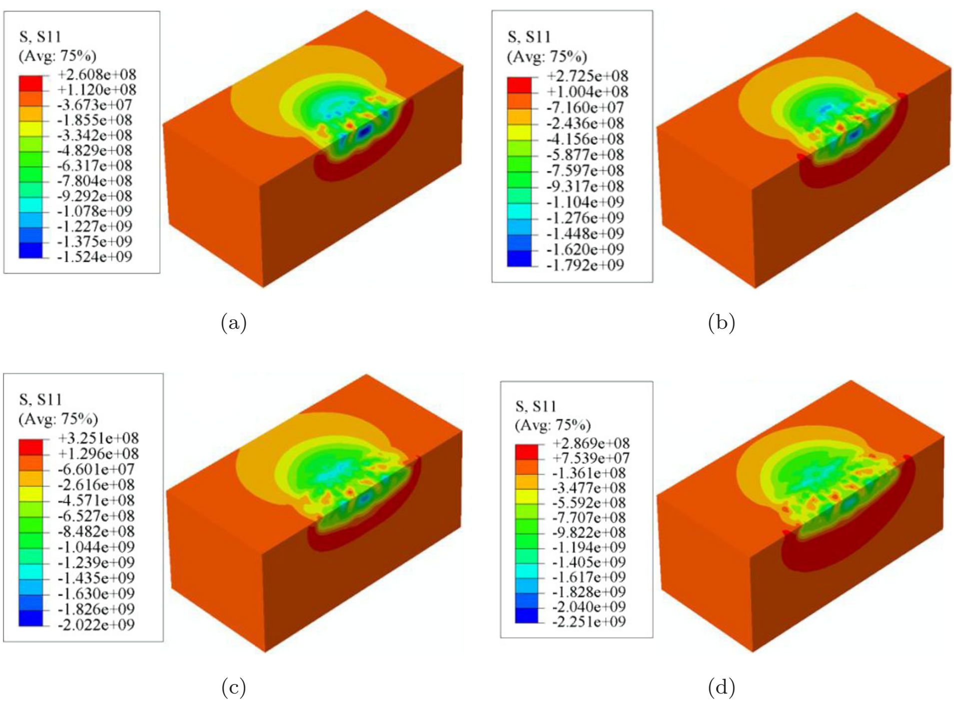

Fig. 7. Close view of the residual stress distributions: (a) 3-shot pattern, (b) 4-shot pattern, (c) 5-shot pattern, and (d) 6-shot pattern.

processed surface. The dilemma can be solved by constructing a new shot group with more number of shots and by sequentially impacting the surface. In the present work, 3-shot, 5-shot, and 6-shot groups were added to the model in addition to 2-shot and 4-shot groups, as shown in Fig. 3. The combination of impacts of various shot groups with different positions significantly expanded the area of the impacted region. Notably, the simulated coverage of the symmetry cell was relatively small (usually 20–43%) by using the coverage equation for random impact simulation [Gangaraj *et al.* (2014)]. The key obstacle was the area of the impacted surface.

It is well known that compressive residual stresses are induced by surface plastic deformation in the shot peening process. Figure 7 shows a close view of the residual stress distributions along the x-axis ($S11$) in the cross-section of the models. It can be observed that blue areas with compressive stress concentration apparently appear in the cross-sections for the 3-shot pattern. The number and volume of blue areas decrease with the increase in the numerical order of shot patterns. When the numerical order reaches 6, the blue area with stress concentration diminishes and a uniform state of stress is obtained. Figure 8 shows the residual stress ($S11$) of the surface nodes along the x-axis in the impacted region for the models. For the 3-shot pattern, some sudden changes can be observed in the stress curve. By increasing the numerical order of shot patterns, the sudden changes gradually disappear and the curve becomes smooth. It can be concluded that the surface residual stress ($S11$) in the impacted region is in a uniform state when the shot number of the shot group reaches 4.

The distributions of PEEQ and residual stress ($S11$) along the depth direction at location K are shown in Fig. 9. The location K was randomly taken in the impact region which is shown in Fig. 10(a). Due to the location of the last shot impact, the PEEQ and residual stress at center point of impact region were not deliberately selected, which would be led to the value overestimated. It can be observed that plastic strains are induced at the depth of 0–400 μm, and the maximum values of

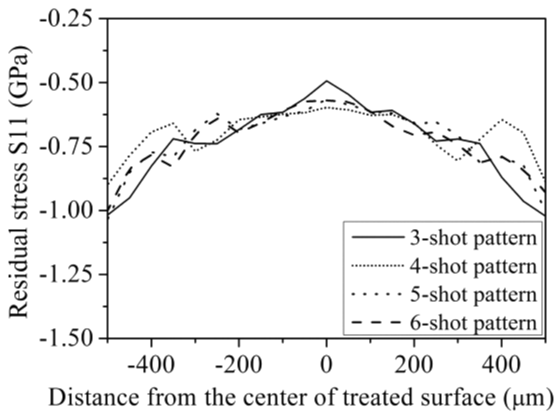

Fig. 8. Residual stress distributions of surface nodes.

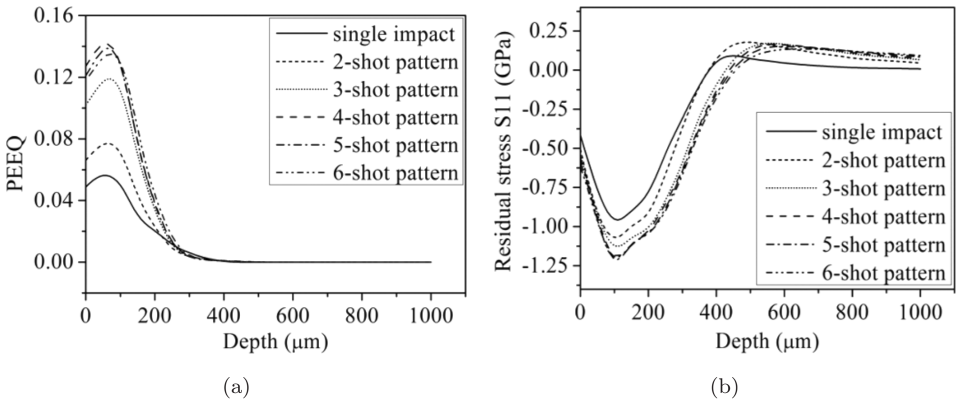

Fig. 9. Simulation results of different shot patterns along the depth direction: (a) PEEQ and (b) residual stress $S11$.

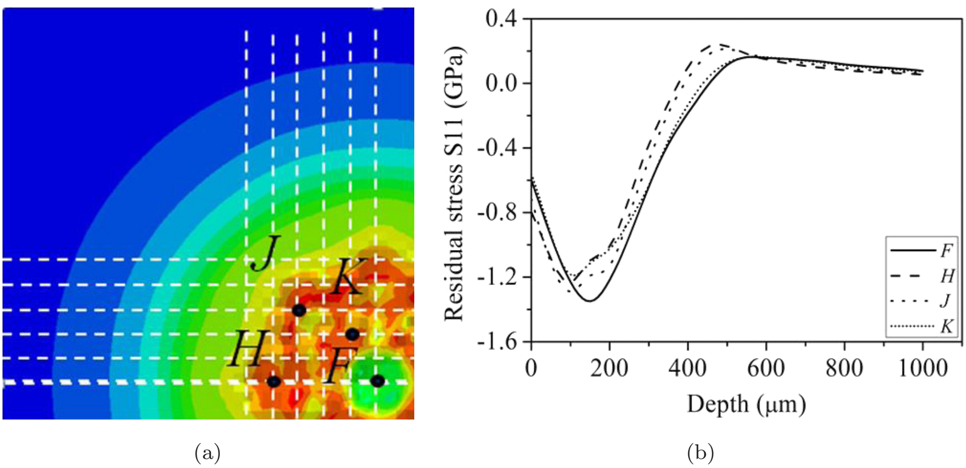

Fig. 10. Residual stress of the 4-shot pattern along the depth direction at four surface points: (a) positions of four points and (b) residual stress $S11$.

PEEQ occur at the depth of approximately $70\,\mu$m. Moreover, the value of PEEQ increases with the increase in the numerical order of shot patterns. Compressive residual stress is introduced in the subsurface of the impacted region and the depth of compressive residual stress is in the range of approximately 0–$400\,\mu$m, which corresponds to the distribution of PEEQ. The value of the residual stress first increases with the increase in the depth and thereafter decreases to almost zero. The maximum value of compressive residual stress increases with the increase in the numerical order of shot patterns, and remains approximately 1.19 GPa when the numerical order of shot patterns reaches 4.

In order to verify the uniform state of stress for the 4-shot pattern, residual stress distributions of four distinct points on the treated surface were studied.

Figure 10(a) shows the positions of four points F, H, J, and K in the von Mises stress distribution on the surface. Point F is located at the center of indentations and the other three points are randomly picked. The residual stress distributions along the depth direction of the four points are shown in Fig. 10(b). It can be observed that each point has an almost similar distribution of residual stress along the depth direction. The maximum magnitude of compressive stress is 1.34 GPa, and the minimum magnitude of compressive stress is 1.19 GPa. The average value of compressive stress is 1.26 GPa, and the standard deviation is 0.07 GPa. Moreover, the maximum compressive stress occurs at the depth of approximately 100–150 μm. Therefore, it can be concluded that the residual stress in the impacted region has a relatively uniform distribution when the 4-shot pattern is applied to the surface.

The FE analysis of the sequential models was performed on a computer with an Intel(R) Core(TM) i3-4150 CPU and 8G RAM, which is a relatively low configuration product. Considering the model of the 4-shot pattern as an example, the calculation takes 44.7 h after 29 impacts of sequential shots with uniform distribution of residual stress in the impacted region. The computational time can be further reduced by using a half-size shot in the model, which shortens the distance from the shots to the treated surface. Compared to the sequential impact model of Majzoobi *et al.* [2005], a uniform state of in-depth residual stress was achieved after the sequential impacts of 25 shots. The particular number of shot impacts is related to the peening conditions. Similarly, the random shot model of Ghasemi *et al.* [2016] requires at least 27 shot impacts for full coverage and to obtain a uniform state of residual stress when the radius of the impacted region is four times the radius of single-shot indentation ($C = 4r$). According to the model of 1000% coverage in the impacted region ($C = 5r$), the simulation requires approximately 80 h. Therefore, the computational efficiency of the proposed sequential model with multiple-shot impacts is comparable to that of other models.

4.2. *Experimental verification*

The residual stresses in the subsurface of GH4169 specimens treated with shot peening were measured using XRD. To reduce the error of measurements, measurements were conducted on center region of three specimens, and the value was obtained from average residual stress. Figure 11 shows XRD measurement of specimen No. 1 including the relationship between the correlation coefficient and diffraction angle 2θ, and the linear fitting of $\sin^2 \Psi$ versus $\Delta 2\theta$. The residual stress measured by XRD can be obtained according to Eq. (1) and the average value is -501.3 MPa, as listed in Table 5. In addition, the residual stress distributions along the depth direction were measured using the incremental hole drilling method. The average residual stress in the subsurface obtained by one-step hole drilling (depth was 50 μm) is -526.5 MPa, as listed in Table 5. Also, Table 5 presents the residual stress in the subsurface obtained using numerical simulation and the value is -567.1 MPa. Notably, the residual stress of simulation was the surface element stress of the 4-shot

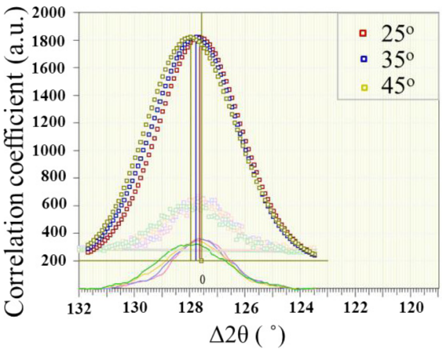

(a)

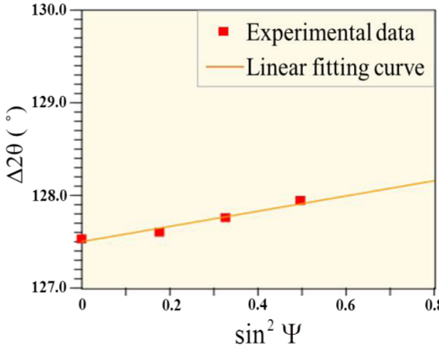

(b)

Fig. 11. XRD measurement of specimen No. 1: (a) offset of correlation coefficient against $\Delta 2\theta$ and (b) linear fitting of $\Delta 2\theta$ and $\sin^2\psi$.

Table 5. Comparison between the numerical calculation and experimental measurements.

Methods	XRD	One step hole drilling method	Numerical simulation
Residual stress (MPa)	-501.3 ± 51.0	-526.5 ± 30.0	-567.1

pattern model. The relative error between the XRD measurement and the numerical result was approximately 11.6%, whereas the relative error between the hole drilling measurement and the numerical result was 7.15%. The results indicate that the numerical calculation is consistent with the experimental measurements.

Figure 12 shows the distribution of residual stresses along the depth direction measured using the incremental hole drilling method, which is also compared with

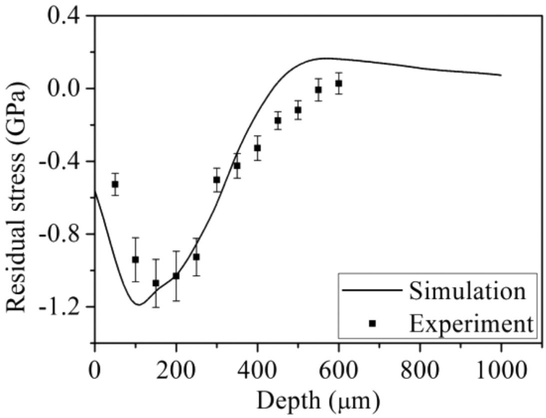

Fig. 12. Residual stress distribution obtained from the incremental hole drilling method and the calculation result of numerical simulation.

the results of the numerical simulation, which was taken at location K point from the model of 4-shot pattern. A good consistency was observed between the experimental results and simulation in the depth profile. The experimental and numerical results of maximum compressive residual stress were 1.07 GPa and 1.19 GPa, respectively, and the corresponding depths were 0.15 mm and 0.12 mm, respectively. The residual stress of measurement was almost zero when the depth of the hole exceeded 0.5 mm. The possible reason may be the small magnitude of residual stress at depths less than 0.5 mm and consequently, the strain gage is less sensitive to the residual stress relaxation as the increments become deeper.

5. Conclusion

A sequential model of multiple-shot impacts was established to investigate the shot peening process of a GH4169 alloy specimen. Compared to traditional sequential models, the proposed model has provided various patterns of shot impact, so that a high surface coverage and a uniform residual stress can be obtained. Moreover, the proposed model has a high computational efficiency in comparison with random models. The conclusions can be summarized as follows:

(1) A sequential model with designed shot groups and shot patterns was proposed to simulate the shot peening process with adequate overlapping and coverage.
(2) The sequential model was applied for the prediction of residual stress on a GH4169 alloy specimen. The results showed that uniform and saturated states of residual stress along the surface and depth profile were obtained in the impacted region when the numerical order of shot patterns reaches 4.
(3) The numerical results for the compressive residual stress in the subsurface were compared with the experimental results obtained using XRD and the incremental hole drilling method. The maximum relative error between the numerical results and XRD measurement was 11.6%. Moreover, the stress profile measured using the incremental hole drilling method was consistent with the numerical results.
(4) This study indicates that the established FE model is robust and effective for the evaluation of residual stress in shot-peened GH4169 alloy. Furthermore, it is also applicable to the estimation of the shot-peened residual stress of other metallic materials with simple modifications.

Acknowledgments

The authors are grateful for financial support from the National Natural Science Foundation of China (Grant No. 11672345), the Natural Science Foundation of Jiangsu Province (Grant No. BK20161341), Six Talent Peaks Project in Jiangsu Province (Nos. 2016-HKHT-004 and 2017-KTHY-010), and Jiangsu Higher Education Institutions Undergraduate Training Programs for Innovation and Entrepreneurship (201810299014Z).

References

Abaqus Analysis User's Manual, Version 6.10.1 released 2010.

ASTM Standard E837 [2008] Standard test method for determining residual stresses by the hole-drilling strain-gage method.

Bagherifard, S., Fernandez-Pariente, I., Ghelichi, R. and Guagliano, M. [2014] "Effect of severe shot peening on microstructure and fatigue strength of cast iron," *Int. J. Fatigue* **65**, 64–70.

Chen, Z., Yang, F. and Meguid, S. A. [2014] "Realistic finite element simulations of arc-height development in shot-peened almen strips," *J. Eng. Mater. Technol.* **136**(4), 041002, doi:10.1115/1.4028006.

Frija, M., Hassine, T., Fathallah, R., Bouraoui, C. and Dogui, A. [2006] "Finite element modelling of shot peening process: prediction of the compressive residual stresses, the plastic deformations and the surface integrity," *Mater. Sci. Eng. A* **426**(1), 173–180.

Gangaraj, S. M. H., Alvandi-Tabrizi, Y., Farrahi, G. H., Majzoobi, G. H. and Ghadbeigi, H. [2011] "Finite element analysis of shot-peening effect on fretting fatigue parameters," *Tribol. Int.* **44**(11), 1583–1588.

Gangaraj, S. M. H., Guagliano, M. and Farrahi, G. H. [2014] "An approach to relate shot peening finite element simulation to the actual coverage," *Surf. Coat. Technol.* **243**(4), 39–45.

Gangaraj, S. M. H., Cho, K. S., Voigt, H. J. L., Guagliano, M. and Schuh, C. A. [2015] "Experimental assessment and simulation of surface nanocrystallization by severe shot peening," *Acta Materialia* **97**, 105–115.

Ghasemi, A., Gangaraj, S. M. H., Mahmoudi, A. H., Farrahi, G. H. and Guagliano, M. [2016] "Shot peening coverage effect on residual stress profile by FE random impact analysis," *Surf. Eng.* **32**(11), 861–870.

Han, K., Peric, D., Crook, A. J. L., Owen and D. R. J. [2000] "A combined finite/discrete element simulation of shot peening processes — part I: Studies on 2D interaction laws," *Eng. Computat.* **17**(5), 593–620.

Hong, T., Ooi, J. Y. and Shaw, B. [2008] "A numerical simulation to relate the shot peening parameters to the induced residual stresses," *Eng. Failure Anal.* **15**(8), 1097–1110.

Huang, X. C., Zhang, D. H., Yao, C. F. and Ren, J. X. [2013] "Effects of grinding parameters on surface integrity of GH4169 Nickel-based superalloy," *J. Aerospace Power* **28**(3), 621–628.

Wang, J. and Liu, F. [2011] "Numerical simulation for shot-peening based on SPH-Coupled FEM," *Int. J. Comput. Methods* **8**(4), 731–745.

Kim, T., Jin, H. L., Lee, H. and Cheong, S. K. [2010] "An area-average approach to peening residual stress under multi-impacts using a three-dimensional symmetry-cell finite element model with plastic shots," *Mater. Des.* **31**(1), 50–59.

Kumagai, M., Akita, K., Imafuku, M. and Ohya, S. I. [2014] "Workhardening and the microstructural characteristics of shot- and laser-peened austenitic stainless steel," *Mater. Sci. Eng. A* **608**, 21–24.

Liu, Z., Wu, N., Huang, X., Xie, H., Lv, X. and He, G. [2012] "Study of anti-laser irradiation performance of shot-peened 40CrNiMoA alloy steel," *Mater. Sci. Eng. A* **558**(48), 675–683.

Mahmoudi, A. H., Ghasemi, A., Farrahi, G. H. and Sherafatnia, K. [2016] "A comprehensive experimental and numerical study on redistribution of residual stresses by shot peening," *Mater. Des.* **90**, 478–487.

Majzoobi, G. H., Azizi, R. and Nia, A. A. [2005] "A three-dimensional simulation of shot peening process using multiple shot impacts," *J. Mater. Process. Technol.* **164–165**(20), 1226–1234.

Meguid, S. A., Shagal, G., Stranart, J. C. and Daly, J. [1999] "Three-dimensional dynamic finite element analysis of shot-peening induced residual stresses," *Finite Elements Anal. Design* **31**(3), 179–191.

Meguid, S. A., Shagal, G. and Stranart, J. C. [2002] "3D FE analysis of peening of strain-rate sensitive materials using multiple impingement model," *Int. J. Impact Eng.* **27**(2), 119–134.

Miao, H. Y., Larose, S., Perron, C. and Lévesque, M. [2009] "On the potential applications of a 3D random finite element model for the simulation of shot peening," *Adv. Eng. Softw.* **40**(10), 1023–1038.

Noyan, I. C., and Cohen, J. B. [1987] "Residual stress: Measurement by diffraction and interpretation," Springer-Verlag, pp. 117–126.

Ochi, Y., Masaki, K., Matsumura, T. and Sekino, T. [2001] "Effect of shot-peening treatment on high cycle fatigue property of ductile cast iron," *Int. J. Fatigue* **23**(5), 441–448.

Ren, X. D., Zhan, Q. B., Yuan, S. Q., Zhou, J. Z., Wang, Y., Ren, N. F., Sun, G. F., Zheng, L. M., Dai, F. Z., Yang, H. M. and Dai, W. J. [2014] "A finite element analysis of thermal relaxation of residual stress in laser shock processing ni-based alloy GH4169," *Mater. Des.* **54**(2), 708–711.

SAE Standard J2277 [2003] Shot peening coverage, developed by Surface Enhancement Committee.

Sanjurjo, P., Rodríguez, C., Peñuelas, I., García, T. E. and Belzunce, F. J. [2014] "Influence of the target material constitutive model on the numerical simulation of a shot peening process," *Surf. Coat. Technol.* **258**, 822–831.

Seddik, R., Bahloul, A., Atig, A. and Fathallah, R. [2017] "A simple methodology to optimize shot-peening process parameters using finite element simulations," *Int. J. Adv. Manuf. Technol.* **90**, 2345–2361.

Sherafatnia, K., Farrahi, G. H., Mahmoudi, A. H. and Ghasemi, A. [2016] "Experimental measurement and analytical determination of shot peening residual stresses considering friction and real unloading behavior," *Mater. Sci. Eng. A* **657**, 309–321.

Soyama, H. and Takeo, F. [2016] "Comparison between cavitation peening and shot peening for extending the fatigue life of a duralumin plate with a hole," *J. Mater. Process. Technol.* **227**, 80–87.

Valentini, E., Beghini, M., Bertini, L., Santus, C. and Benedetti, M. [2011] "Procedure to perform a validated incremental hole drilling measurement: Application to shot peening residual stresses," *Strain* **47**(s1), e605–e618.

Wang, C., Jiang, C. and Ji, V. [2017] "Thermal stability of residual stresses and work hardening of shot peened tungsten cemented carbide," *Journal of Materials Processing Technology* **240**, 98–103.

Wu, L. F., Zhu, J. G. and Xie, H. M. [2014] "Numerical and experimental investigation of residual stress in thermal barrier coatings during APS process," *J. Thermal Spray Technol.* **23**, 653–665.

Wu, L. F., Zhu, J. G. and Xie, H. M. [2015] "Investigation of residual stress in 2D plane weave aramid fibre composite plates using moiré interferometry and hole-drilling technique," *Strain* **51**, 429–443.